Prospective identification, isolation, and systemic transplantation of multipotent mesenchymal stem cells in murine bone marrow

Satoru Morikawa,[1,2] Yo Mabuchi,[1] Yoshiaki Kubota,[3] Yasuo Nagai,[1] Kunimichi Niibe,[1,2] Emi Hiratsu,[1] Sadafumi Suzuki,[1] Chikako Miyauchi-Hara,[1,6] Narihito Nagoshi,[1,4] Takehiko Sunabori,[1] Shigeto Shimmura,[5] Atsushi Miyawaki,[6,7] Taneaki Nakagawa,[2] Toshio Suda,[3] Hideyuki Okano,[1] and Yumi Matsuzaki[1]

[1]Department of Physiology, [2]Department of Dentistry and Oral Surgery, [3]Department of Cell Differentiation, the Sakaguchi Laboratory of Developmental Biology, [4]Department of Orthopedic Surgery and [5]Department of Ophthalmology, Keio University School of Medicine, Shinjuku-ku, Tokyo 160-8582, Japan
[6]Laboratory for Cell Function and Dynamics, Advanced Technology Development Group, Brain Science Institute, Institute of Physical and Chemical Research, Wako-city, Saitama 351-0198, Japan
[7]Life Function and Dynamics, Exploratory Research for Advanced Technology Office, Japan Science and Technology Agency, Wako-city, Saitama 351-0198, Japan

Mesenchymal stem cells (MSCs) are defined as cells that undergo sustained in vitro growth and can give rise to multiple mesenchymal lineages. Because MSCs have only been isolated from tissue in culture, the equivalent cells have not been identified in vivo and little is known about their physiological roles or even their exact tissue location. In this study, we used phenotypic, morphological, and functional criteria to identify and prospectively isolate a subset of MSCs (PDGFRα$^+$Sca-1$^+$CD45$^-$TER119$^-$) from adult mouse bone marrow. Individual MSCs generated colonies at a high frequency and could differentiate into hematopoietic niche cells, osteoblasts, and adipocytes after in vivo transplantation. Naive MSCs resided in the perivascular region in a quiescent state. This study provides the useful method needed to identify MSCs as defined in vivo entities.

CORRESPONDENCE
Yumi Matsuzaki:
penguin@sc.itc.keio.ac.jp

Abbreviations used: BLI, bioluminescence imaging; BMMNC, BM mononuclear cell; CFU-F, fibroblast CFU; CFU-S, spleen CFU; HSC, hematopoietic stem cell; IHC, immunohistochemistry; mMSC, murine MSC; MPC, mesenchymal progenitor cell; MSC, mesenchymal stem cell; PDGFRα, platelet-derived growth factor receptor α; Sca-1, stem cell antigen 1; vSMC, vascular smooth muscle cell.

Adult BM is composed of hematopoietic stem cells (HSCs) and tissue stem cells, which are often referred to as fibroblast CFUs (CFU-Fs), marrow stromal cells/mesenchymal stem cells (MSCs), or mesenchymal progenitor cells (MPCs; Friedenstein et al., 1974; Prockop, 1997; Conget and Minguell, 1999; Pittenger et al., 1999). As information is gathered about MSCs, parallels are often drawn between them and the extensively characterized HSCs. HSCs were initially identified by Till and McCulloch (1961), who called them spleen CFUs (CFU-Ss), and MSCs were first described by Friedenstein et al. (1974), who called them CFU-Fs. There has since been a major divergence in the way the two stem cell types are studied.

HSCs can be identified prospectively by surface markers, isolated by flow cytometry, and transplanted in vivo without being cultured in vitro (Smith et al., 1991; Spangrude et al., 1995; Osawa et al., 1996; Matsuzaki et al., 2004). In contrast, MSCs, which can give rise to multiple mesenchymal cell lineages, including adipocytes, chondrocytes, and osteocytes (Prockop, 1997; Pittenger et al., 1999), are currently isolated by culturing tissues from humans and other species (da Silva Meirelles et al., 2006; Beltrami et al., 2007). Therefore, most information about MSCs comes from in vitro studies (Pittenger et al., 1999) of heterogeneous populations of adherent cells that contain unidentified, putative stem cells. This is a critical difference because it is the ability to isolate HSCs prospectively that has facilitated the rapid

The Rockefeller University Press $30.00
J. Exp. Med. Vol. 206 No. 11 2483-2496
www.jem.org/cgi/doi/10.1084/jem.20091046

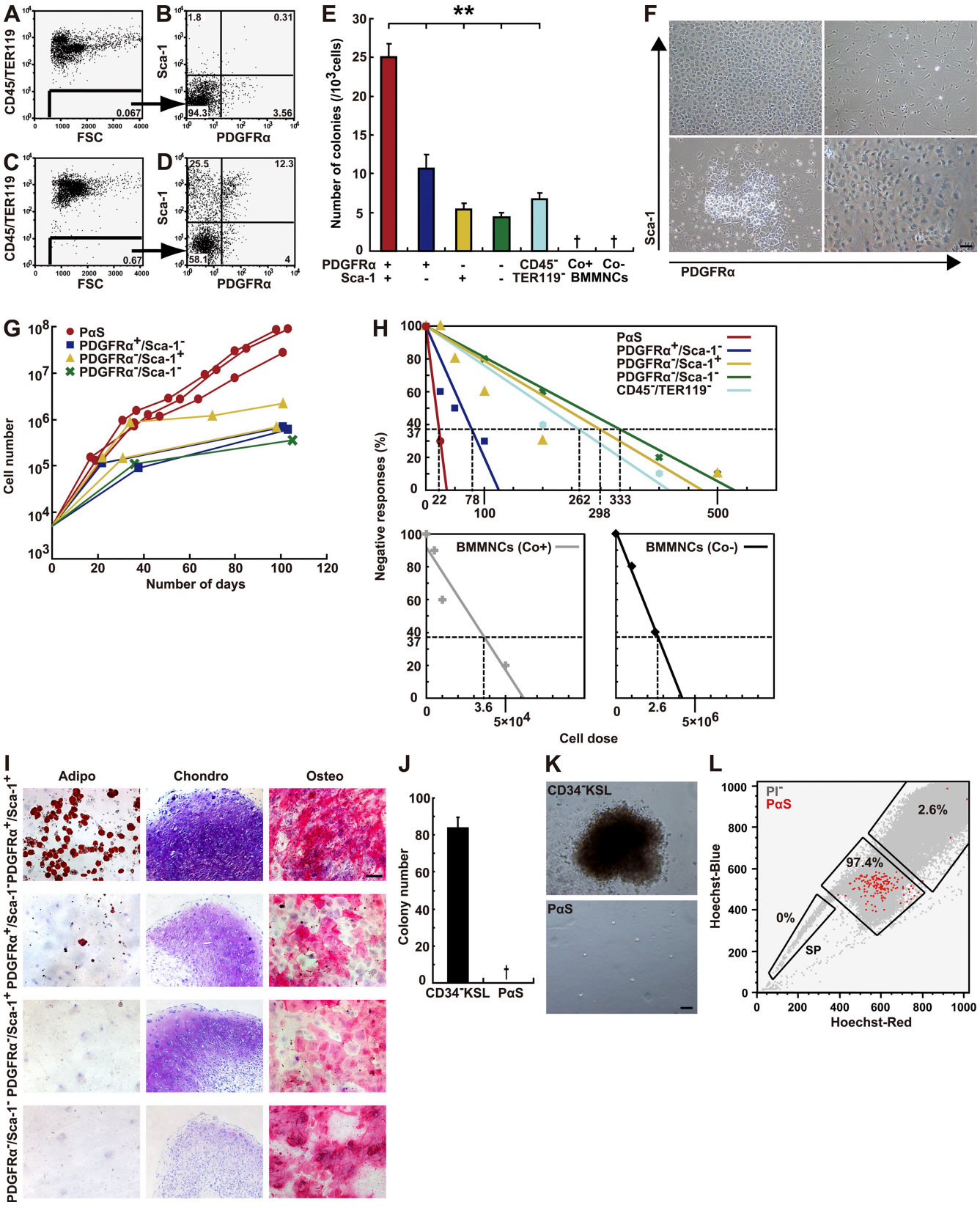

Figure 1. Enrichment of mesenchymal stem cells in the PαS population. (A–D) Representative flow cytometric profiles of BM mononuclear cells stained with CD45, TER119, PDGFRα, and Sca-1 without (A and B) or with (C and D) collagenase treatment. (E) Number of CFU-Fs 14 d after plating. Data

progress in understanding their biology. In contrast, because our knowledge of MSCs is based solely on the characterization of cultured cells, it has been virtually impossible to study many of their properties, particularly their function, in vivo.

Recent studies consistently show that MSCs not only differentiate into mesenchymal lineage cells but also into neurons (Kohyama et al., 2001; Kondo et al., 2005), skeletal muscle (Dezawa et al., 2005), and myocardium (Makino et al., 1999; Miyahara et al., 2006). Therefore, MSCs are now considered a potentially effective source for stem cell therapy (Jin et al., 2002; Hoffmann et al., 2006). However, safety issues still need to be clarified before their clinical use, particularly because so many biological aspects of MSCs, such as their exact identity and in vivo function, are still unknown.

One disadvantage of the conventional in vitro method for isolating MSCs is the unavoidable contamination by hematopoietic cells and the cellular heterogeneity of the cultures, including various fibroblastic cells. In fact, depending on the study, cultured MSCs express a different subset of various cell lineage–specific antigens, adhesion molecules, integrins, and growth factor receptors (Jiang et al., 2002; da Silva Meirelles et al., 2006). Another problem with the current technique is that the cultured cells may acquire different characteristics from their in vivo state, which could include changes in the cell surface markers they express. One example of adherent culture-induced change is seen when MSCs, which are readily expanded in culture without loss of multipotency, show poor tissue tropism when transplanted, including a failure to migrate to the BM (Rombouts and Ploemacher, 2003; Wang et al., 2005; Muguruma et al., 2006; Sackstein et al., 2008), which limits their therapeutic usefulness. In contrast, some studies (including the current one) show that primary BM-derived MSCs (assayed as CFU-Fs) show a low but efficient seeding of the BM upon injection into lethally irradiated hosts (Rombouts and Ploemacher, 2003; Koide et al., 2007). Because these changes affect fundamental properties of the cells, it is difficult to know whether they have retained or lost their original characteristics, including their apparent multipotency, in vitro.

Most studies on MSCs have been done using human cells, not murine cells. Murine MSCs (mMSCs) are far more difficult to isolate from the BM and to expand in culture than human MSCs (Phinney et al., 1999; Sun et al., 2003; Peister et al., 2004). Thus, there is much less information on mMSCs than on human MSCs. This reliance on human material means that MSCs cannot be studied in genetic mouse models, which greatly hinders the study of their basic biology, engraftment, and therapeutic potential. In fact, without some means for the prospective isolation and purification of MSCs, it becomes extremely difficult to ascribe any attribute to them with certainty. Hence, there is a clear need for specific markers and methods of detection, enumeration, and isolation of MSCs from the BM and other tissues where they reside.

In a previous study, we identified several mesenchymal lineage specific markers in murine BM cells (Koide et al., 2007), and after initial screening, we determined two possible MSC markers (Morikawa et al., 2009), platelet-derived growth factor receptor α (PDGFRα; an early mesodermal marker; Takakura et al., 1997) and stem cell antigen-1 (Sca-1; a known stem cell marker; Ortega et al., 1986).

Here, we report a method for identifying and isolating MSCs from the adult murine BM, using flow cytometry in combination with in vitro function assays. We also report our findings on their physiological role, obtained through existing in vivo precursor cell transplantation assays. We describe cell type–specific markers for MSCs, which are useful for their prospective isolation as a highly enriched population that gives rise to mesenchymal cells at the clonal level with high frequency, and demonstrate that these cells are capable of in vivo grafting when transplanted systemically.

RESULTS

The PαS population is significantly enriched for CFU-Fs with differentiation potential

Freshly prepared BM cells were stained with antibodies to PDGFRα, Sca-1, CD45, and TER119, and analyzed by flow cytometry. First, the hematopoietic ($CD45^+$ and $TER119^+$) cells were removed from the population by gating on the marker signals (Fig. 1, A and C). In the $CD45^-TER119^-$ gate, four distinct subpopulations ($PDGFR\alpha^+/Sca\text{-}1^+$, $^{+/-}$, $^{-/+}$, $^{-/-}$) were observed (Fig. 1 B). Interestingly, the frequency of cells expressing PDGFRα or Sca-1 significantly increased when the BM was extracted using collagenase treatment (Fig. 1, B and D; see Materials and methods).

To test whether PDGFRα or Sca-1 could be used for the prospective isolation of mMSCs, we isolated cells in each subpopulation from freshly isolated BM mononuclear

are mean ± SEM (n = 3 per group; **, $P < 0.01$; †, no colonies observed). (F) Phase-contrast micrographs of CFU-Fs 14 d after plating, derived from 5,000 $PDGFR\alpha^-Sca\text{-}1^+$, $PDGFR\alpha^+Sca\text{-}1^+$, $PDGFR\alpha^+Sca1^-$, or 1×10^4 $PDGFR\alpha\text{-}Sca\text{-}1^-$ cells. (G) Growth curves of representative populations derived from 5,000 cells plated. (H) Negative linear relationship between the number of subpopulation BM cells seeded and the proportion of negative colony formation obtained by three independent experiments. (I) Adipogenesis (left) was indicated by neutral lipid vacuoles that stained with oil red O on day 14. Chondrogenesis (middle) indicated by toluidine blue staining on day 21 and by morphological changes. Osteogenesis (right) indicated by alkaline phosphatase staining on day 14. (J) CFU-Cs assays. PαS cells (5,000) and $CD34^-$ KSL cells (100) were seeded into separate cultures with MethoCult medium. The total numbers of colonies counted at 14 d are shown. †, no colonies observed. (K) Phase-contrast micrograph of a representative colony derived from $CD34^-$ KSL cells (top). No colonies arose from PαS cells under this condition (bottom). Bars, (F, I, and K) 100 µm. (L) Two-dimensional flow cytometric profile of the Hoechst-Red and Hoechst-Blue fluorescence intensity of PI-negative cells (gray) and PαS cells (red). Data are representative of three independent experiments.

cells (BMMNCs) and performed several in vitro assays to determine their characteristics. A traditional CFU-F assay showed that the number of colonies per 1,000 cells was highest in the PDGFRα$^+$Sca-1$^+$CD45$^-$TER119$^-$ (PαS) subpopulation; however, the cells in the other subpopulations still produced a significant number of colonies (Fig. 1 E). Conventional MSC culture conditions (Phinney et al., 1999; Pittenger et al., 1999) yielding fibroblastic/spindle-shaped cells indicative of MSCs were only derived in the PαS cultures on day 14 (Fig. 1 F, top right). The other subpopulations showed different morphologies, such as the cobblestone appearance typical of endothelial cells, observed in the PDGFRα$^-$Sca-1$^+$ group (Fig. 1 F). In addition, an analysis of growth kinetics revealed that only the PαS cells proliferated without senescence, yielding more than 10^7 cells from the original 5,000 cells seeded, with a doubling time of 50.6 h (Fig. 1 G).

We also observed a negative linear relationship between seeding density and colony formation efficiency (Fig. 1 H; Stingl et al., 2006). In unfractionated BMMNCs, isolated without collagenase treatment, the frequency of CFU-Fs was $1/2.6 \times 10^6$ cells, as described previously (Phinney et al., 1999). It was 100 times greater when collagenase treatment was used ($1/3.6 \times 10^4$). The frequency of CFU-Fs obtained from PαS cells was 1 per 22.5 cells, which was consistent with the bulk CFU-F assays (Fig. 1 E). Collectively, the PαS cells showed a 120,000-fold higher CFU-F frequency than the unfractionated BMMNCs.

The PαS cells' potential for in vitro mesenchymal lineage differentiation was also investigated (Fig. 1 I). Freshly prepared BM cells were separated into the four CD45$^-$TER119$^-$ subpopulations described above, cultured with maintenance media for one or two passages, and then grown in differentiation-induction media for an additional 14–21 d. Only the PαS cells differentiated robustly into adipocytes, chondrocytes, and osteocytes. Although other fractions formed a pelletable micro-mass when grown under chondrogenic conditions, the extracellular matrix was either scarce or absent, as tested by toluidine blue staining. Adipocytes were generated almost solely by the PαS population, although a very few were occasionally seen in the PDGFRα$^+$Sca-1$^-$ population. PαS cells were also detected in the BM of other mouse strains, and showed both high colony-forming frequency and trilineage differentiation potential at levels comparable to the C57BL/6 PαS cells (Fig. S1).

As might be expected for MSCs, the PαS cells did not have any hematopoietic capacity in vitro. They did not contain any CFUs under hematopoietic culture conditions, whereas sorted HSCs (CD34$^-$KSL cells) formed over 80 colonies per 100 cells under the same conditions (Fig. 1, J and K). Notably, flow cytometric analysis showed that the PαS BM fraction did not contain any side population (SP) cells, a population enriched for stem cells, including HSCs, derived from a variety of tissues (Fig. 1 L; Goodell et al., 1996; Ono et al., 2007; Oyama et al., 2007).

A single, self-renewing PαS cell can give rise to mesenchymal and endothelial lineages

To test the hypothesis that PαS cells contained MSCs that could differentiate into all three lineages, and to rule out the possibility that the PαS population contained several different kinds of committed progenitors, we performed a differentiation assay with expanded cell colonies derived from a single PαS cell. For this experiment, sorted PαS cells were plated at a density of ~$1\text{-}2 \times 10^3$ cells on a 100-mm dish. 60 individual colonies of 50–100 cells were isolated ~14 d after plating (Fig. 2 A). After several passages, 6 of the 60 independent clones were selected for further study and subjected to in vitro differentiation assays.

All six clones showed osteogenic and chondrogenic differentiation, assessed by alkaline phosphatase/toluidine blue staining and the expression of bone and cartilage-related genes, including *osteopontin*, *osteocalcin*, *PTHr*, *collagen II*, *collagen X,* and *aggrecan*. Four (clones 7, 11, 17, and 19) also underwent adipogenic differentiation, demonstrated by oil red O staining and the expression of fat-related genes, including *adipsin*, *PPARγ*, and *mLP* (Fig. 2, B and C). Interestingly, these four clones also underwent angiogenic differentiation, as shown by staining for endothelium-associated proteins (PECAM-1 and VE-cadherin). These results suggest that MSCs are precursors for both mesenchymal and endothelial lineages.

Flow cytometric analysis of clones from single cells revealed uniform expression of conventional mesenchymal markers CD29, CD49e, CD44, and Sca-1, but only heterogeneous expression of CD105 and CD90, which are known as marker for cultured human MSCs. Clones with multilineage differentiation potential (#7, 11, 17, and 19) were CD105$^+$CD90$^+$, unlike those with limited differentiation potential (#26, 42). This observation suggests that CD105 and CD90 may be useful indicators for multipotency of cultured mMSCs (Fig. S2).

PαS cells reside in the perivascular space in vivo

The data presented so far convinced us that the PαS population represented primary mMSCs. Therefore, we further investigated the in vivo localization and cell-surface phenotype of naive PαS cells by whole-mount immunohistochemistry (whole-mount IHC) and flow cytometry. As far as we observed in >100 microscopic fields of three individual wild-type C57BL/6, all PαS cells were located in the arterial perivascular space near the inner surface of the cortical bone (Fig. 3 A), adjacent to vascular smooth muscle cells (vSMCs) in BM (Fig. 3 B). PDGFRα was expressed in a broader cell population that included cells with reticular morphology, and relatively weak Sca-1 expression was detected in the endothelial cells (Fig. 3 B).

Because reticular cells located in the perivascular space act as hematopoietic niche cells (Sugiyama et al., 2006), we used quantitative RT-PCR (Fig. 3 C) and IHC (Fig. 3 D) to examine the expression of two major paracrine factors that maintain hematopoiesis: angiopoietin-1 (*Ang-1*; Arai et al., 2004) and CXCL12 (Sugiyama et al., 2006). We found abundant

expression of *Ang-1* in the PαS cells and of *CXCL12* in the PDGFRα^{+}Sca-1^{-} cells, suggesting that the MSCs constitute a hematopoietic niche in the arterial perivascular area near the endosteum (Moore and Lemischka, 2006).

Flow cytometric analysis of fresh BMMNCs (Fig. 3 E) revealed that PαS cells uniformly expressed known markers for cultured human MSCs (CD29, CD49e, CD105, CD133, and PDGFRβ). Endothelial cell markers (Flk-1, VEGFR3, and CD146, except for CD34) were also uniformly expressed, although the fluorescence intensities were lower than that of the markers for cultured human MSCs. Markers for HSCs (c-kit and CD150) were totally negative. The cells showed

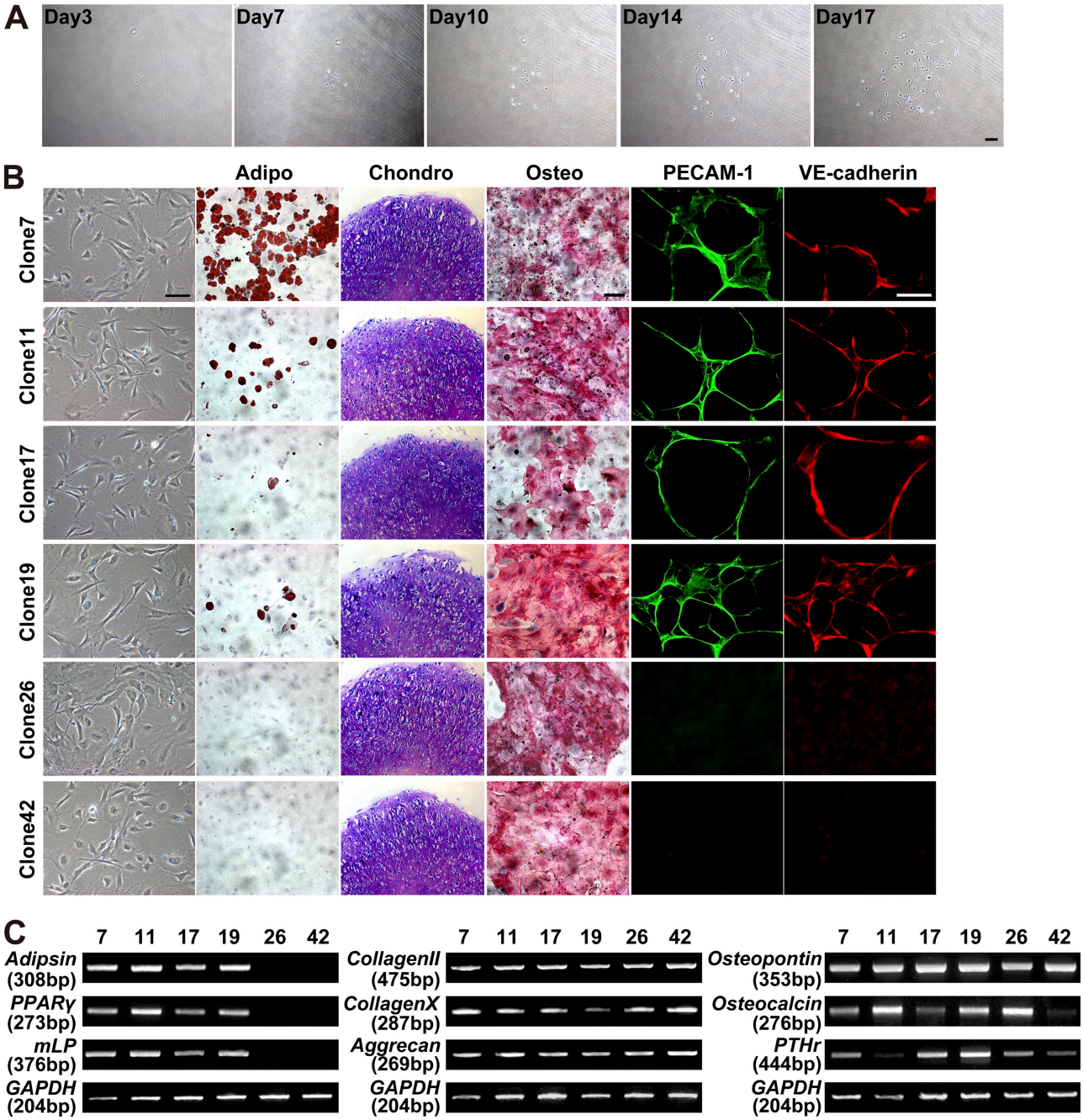

Figure 2. Identification of MSC potential by clonal assay. (A) Phase-contrast micrographs of a representative colony from a single PαS cell. Bar, 200 µm. (B) Comparison of the differentiation potential of clonally derived cells. Adipogenic (day 14), chondrogenic (day 21), osteogenic (day 14), and endothelial (anti-PECAM-1^{+} and VE-cadherin^{+}, day 21). Bars, 100 µm. (C) RT-PCR analysis of transcription factors and lineage-specific genes. Expression of adipocyte- (*Adipsin*, *PPARγ*, and *mLP*), chondrocyte- (*CollagenII*, *CollagenX*, and *Aggrecan*), and osteocyte-specific (*Osteopontin*, *Osteocalcin*, and *PTHr*) markers, 3 wk after differentiation induction. Data are representative of five independent experiments.

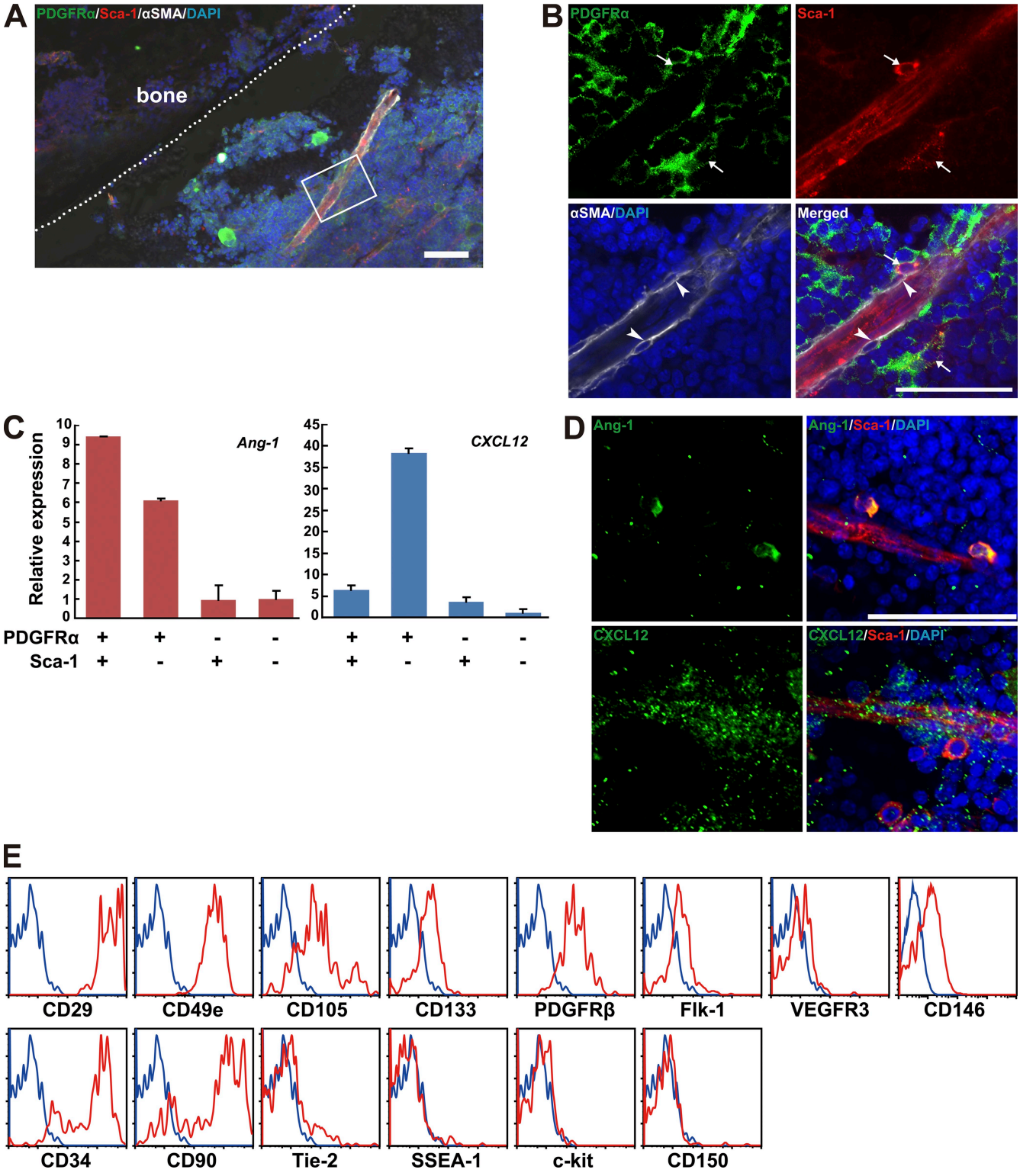

Figure 3. In vivo localization and phenotype of PαS cells. Whole-mount IHC was performed in bone marrow from wild-type C57BL/6 animals. (A) Representative results for quadruple IHC of PDGFRα (green), Sca-1 (red), αSMA (white), and DAPI (blue) in untreated bone marrow. (B) High magnification image of the boxed area in A. PαS cells (arrows), vascular smooth muscle cells (arrowheads). Data are representative of three independent recipients. (C) Quantitative RT-PCR analysis of *Ang-1* and *CXCL12*. The expression levels detected in PDGFRα$^-$ Sca-1$^-$ cells were defined as 1 for each experiment. Mean ± SEM; $n = 6$ per group. (D) Triple IHC of Sca-1 (red), DAPI (blue), and Ang-1 (green, top left) or CXCL12 (green, bottom left). Data are representative of three independent recipients. (E) Representative results of flow cytometric analysis for cell-surface markers by using freshly isolated BMMNCs from wild-type C57BL/6 animals of three independent experiments. Blue line, isotype control; red line, specific antibodies. Bars: (A, B, and D) 50 µm.

heterogeneous expression of the endothelial cell marker CD34, cultured MSC marker CD90, and endothelial cell/HSC marker Tie-2.

PαS cells repopulate hematopoietic niche components and adipose tissue in vivo

Although the transplantation of mesenchymal stem cells has not been believed to be feasible (Wang et al., 2005; Sackstein et al., 2008), we and several other groups have reported that freshly isolated BM cells can replace a part of mesenchymal or stromal cells (Hou et al., 1999; Pereira et al., 1998; Rombouts and Ploemacher, 2003; Koide et al., 2007). To examine whether naive MSCs can reconstitute the BM in vivo, freshly isolated 10^4 PαS cells from CAG-EGFP transgenic mice ($EGFP^+$ $CD45.1^-$) were intravenously injected into lethally irradiated recipient mice ($EGFP^-$ $CD45.1^-$) along with 100 $CD34^-KSL$ cells (HSCs sorted from $EGFP^-$ $CD45.1^+$ mice; Fig. 4). The cells derived from PαS or HSCs were traceable by their expression of EGFP or CD45.1, respectively.

At 16 wk, the peripheral blood of 10 out of 10 recipients had been reconstituted by HSC-derived CD45.1-positive cells averaging 81.1 ± 4.9% of the total cells counted (unpublished data). The recipient animals were subsequently sacrificed and BM sections were subjected to whole-mount IHC. We found a significant number of PαS-derived GFP^+ cells in the BM and surrounding bone tissue in all recipients. The majority of the cells were located in the perivascular region or apposing the inner-surface of cortical bone (Fig. 4 A). Double IHC for GFP and marker molecules revealed that the transplanted PαS cells differentiated into reticular cells in association with vSMCs (Fig. 4 B, a–c), consistent with the normal physiological localization of PαS cells (Fig. 3, A and B). The CXCL12 (Fig. 4 B, d–f) and Ang-1 (Fig. 4 B, g–i) expression in these cells suggested they could reconstitute the vascular niche for hematopoiesis. GFP-positive PαS cells had also differentiated into osteocalcin-expressing osteoblasts lining the inner surface of the cortical bone (Fig. 4 B, j–l). In addition, in the adipose tissue of recipient mice we found some GFP-positive cells that were also positive for perilipin (Fig. 4 B, m–o), an adipocyte marker that is specifically expressed at the periphery of lipid droplets (Cho et al., 2007). Combined with the localization of naive PαS cells in BM shown in Fig. 3 (A–D), these data suggested that within 16 wk of systemic transplantation, primary PαS cells (MSCs), which are normally located in the arterial perivascular space in association with vSMCs, can give rise to osteoblasts and perivascular cells that function as hematopoietic niche cells (Fig. S3) or produce adipocytes when the cells migrate to adipose tissue.

However, systemically transplanted GFP^+ MSCs derived from single PαS cells in culture were not detectable 8 wk later. To investigate this further, 10^5 1-mo-culture–expanded PαS cells that had been engineered to express firefly luciferase fused to Venus (see Materials and methods) were transplanted into lethally irradiated recipient mice. The animals were subjected to bioluminescence imaging (BLI) analysis (Okada et al., 2005)

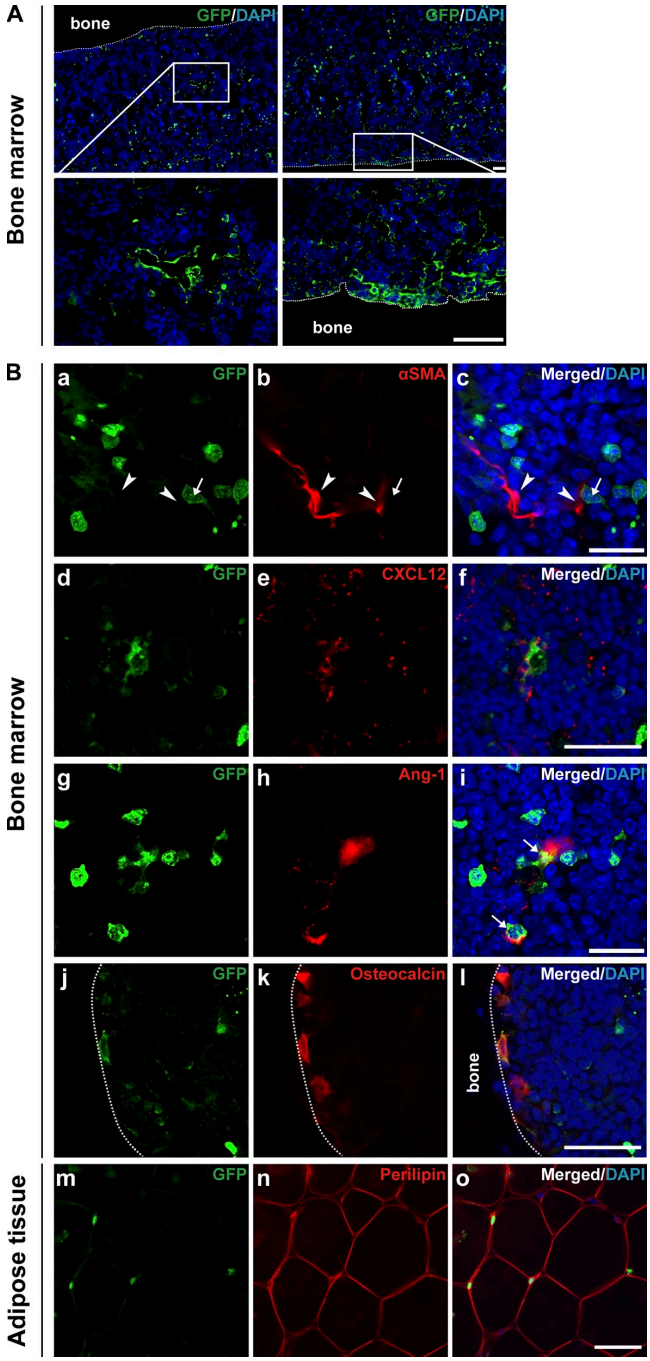

Figure 4. Multilineage capacity of transplanted PαS cells in vivo. Representative pictures of bone specimens from lethally irradiated wild-type C57BL/6 mice ($EGFP^-$ $CD45.1^-$; $n = 5$ mice in three independent experiments), 16 wk after the intravenous transplantation of 10^4 PαS cells from CAG-EGFP transgenic mice BMMNCs ($EGFP^+$ $CD45.1^-$) and of 100 $CD34^-KSL$ cells from B6-Ly5.1 ($EGFP^-$ $CD45.1^+$) mice. (A) The boxed areas in the top panels are shown enlarged in the bottom panels. Bars: (top) 100 µm; (bottom) 50 µm. (B) Double IHC of GFP (green; a, d, g, j, and m) and either αSMA (red; b and c), CXCL12 (red; e and f), Ang-1 (red; h and i), osteocalcin (red; k and l), or perilipin (red; n, o). Nuclei were stained with DAPI (blue; c, f, i, l, o). Note the GFP^+ cells (arrows) differentiated into perivascular cells expressing CXCL12, osteoblasts, or adipocytes, but not vSMCs (arrowheads). Bars: (c and i) 20 µm; (f, l, o) 50 µm.

on days 0, 1, 3, 7, and 14 after transplantation. Strong bioluminescent signals in the bilateral lung and neck were observed on days 0, 1, and 3, but the signals attenuated below the level of detectability by day 7 (Fig. S4). The data strongly support a previous observation that MSCs rapidly lose their ability to home to an appropriate site when cultured (Rombouts and Ploemacher, 2003; Wang et al., 2005).

We further investigated whether transplanted PαS cells maintained their stem cell properties by observing whether secondary CFU-Fs could be clonally expanded, which would indicate their competence for self-renewal. At 16 wk after transplantation, the bone and BM of five recipient mice were individually collagenase digested into single-cell suspensions. Flow cytometric analysis showed that donor-derived GFP$^+$ nonhematopoietic (CD45$^-$TER119$^-$) cells (Fig. 5 A, left) were <10% (mean percentage 7.35%), although the percentage varied in all cases. Notably, GFP$^+$ cells belonging to populations other than PαS were found (Fig. 5 A, right). To test

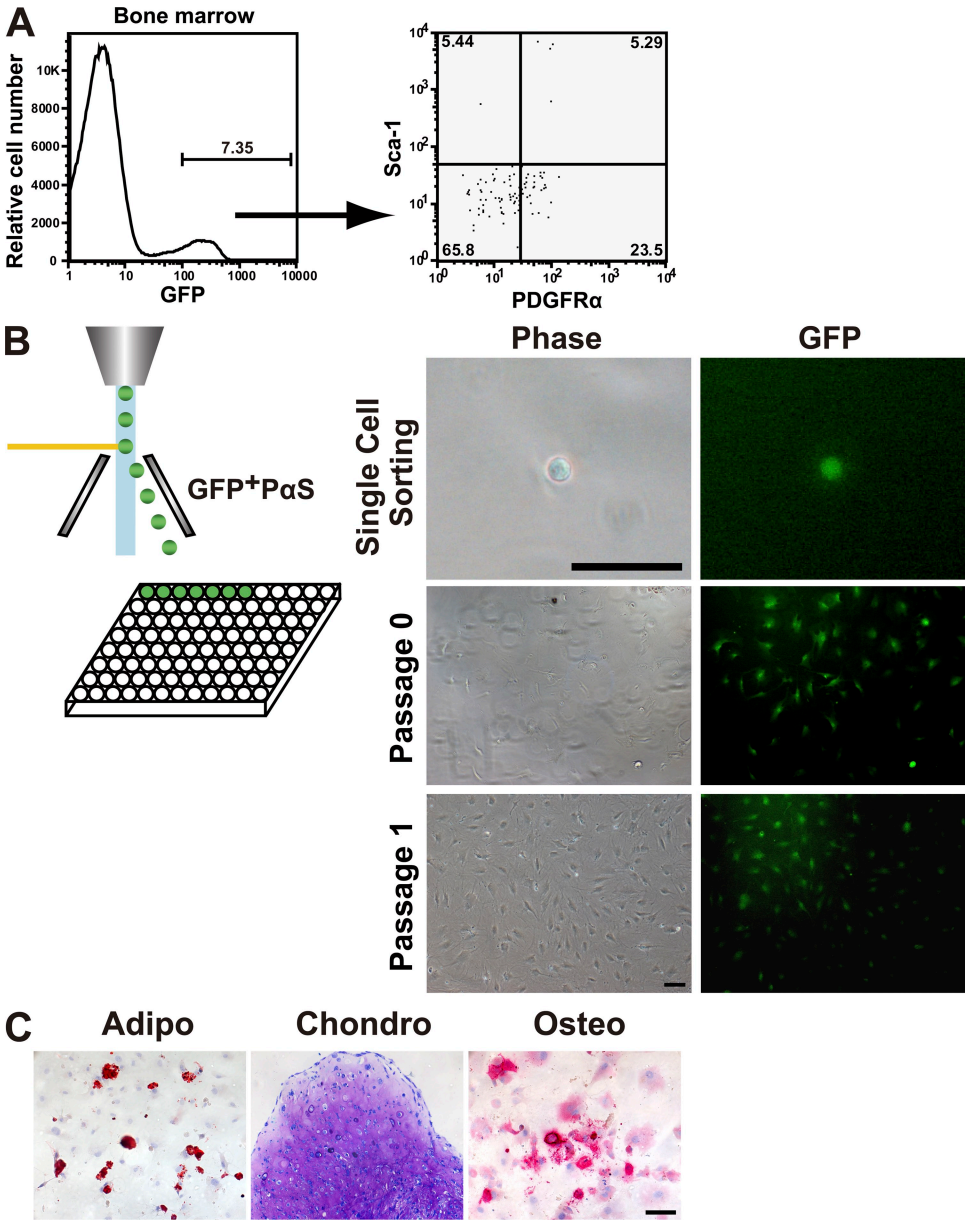

Figure 5. Self-renewal and differentiation capacity of transplanted PαS cells. Wild-type B6 animals were intravenously transplanted with freshly isolated 10^4 PαS cells. (A) Representative result from flow cytometric analysis of EGFP expression of BMMNCs in recipient mice ($n = 5$ mice in three independent experiments) at 16 wk after transplantation. (B) PαS cells from five recipients were then single sorted by flow cytometry and cultured individually in 96-well tissue culture plates. Bar, 50 µm. Colonies were formed by the sorted single PαS, which were able to sustain proliferation in vitro. Bar, 100 µm. (C) GFP$^+$ PαS clones derived from transplanted PαS were multipotent and could give rise to adipocytes (left; oil red O staining, day 14), chondrocytes (middle; toluidine blue staining, day 21), and osteocytes (right; alkaline phosphatase staining, day 14). Bar, 100 µm.

if the recovered PαS cells retained their stem cell properties, we sorted single PαS cells into individual wells of 96-well plates, and analyzed the resulting colonies. GFP^+ fibroblastic colonies generated from 2 of 96 cells (Fig. 5 B), and the 2 clones retained the ability to undergo sustained growth, as well as the multilineage differentiation potential in vitro (Fig. 5 C).

PαS cells are resistant to whole-body irradiation

Although our data showed that the prospectively isolated PαS cells (primary MSCs) migrated to appropriate sites and differentiated into the expected cell types after systemic infusion, the mean chimerism resulting from the transplantation of 10^4 PαS-derived cells was ~7%. In contrast, 100 purified HSCs were sufficient to reconstitute >80% of the hematopoietic cells (Fig. 6 A). Given that 10^4 PαS cells contained ~500 CFU-Fs, based on our 1/20 frequency of CFU-Fs in PαS cells (Fig. 1 H), the PαS engraftment was lower than expected. The observed difference might have been caused by the irradiation protocol. That is, if the recipient's MSCs had not been eliminated in sufficient numbers to leave their niche available to the donor MSCs, competition for the niche might have reduced the number of successfully engrafted cells (Rombouts and Ploemacher, 2003; Koide et al., 2007). To evaluate this hypothesis, we compared the susceptibility of HSCs (KSL) and MSCs (PαS) to irradiation.

Three mice in each group were subjected to whole-body irradiation at a dose of 10.5 Gy, a significant number of PαS cells remained among the BMNNCs after 6 d, but the HSCs (KSL cells) were almost undetectable by flow cytometry (Fig. 6, B and D). Interestingly, the sorted PαS cells from the irradiated animals mostly failed to form colonies, and the CFU-F frequency was reduced to 1.66 ± 0.57% (33 ± 5.0% in unirradiated; Fig. 6 C). Because irradiation normally induces cell death in actively cycling cells, we reasoned that the MSC/PαS cells were quiescent. Flow cytometric analysis for cell-cycle markers showed that 71% of freshly isolated PαS cells were in the G_0 phase (Fig. 6 E), which could have protected them from lethal irradiation. These findings suggest that a significant proportion of the PαS cells are physiologically quiescent and therefore resistant to radiation damage and myelotoxicity in vivo.

DISCUSSION

Using cell-surface markers and flow cytometry, we succeeded in prospectively isolating MSCs as $PDGFR\alpha^+Sca\text{-}1^+CD45^-TER119^-$ (PαS) cells from adult murine BM. We showed that PαS cells have primitive characteristics consistent with conventional MSC populations isolated by adhesion culture. Because PαS cells were detected in various mouse strains (Fig. S1) with equal CFU-F frequency and differentiation potency, our protocol has immense potential for isolating enriched, primary MSCs for detailed analyses especially in various genetically modified animals. Unlike with conventional protocols, our protocol permits such studies to be done with minimal contamination by unnecessary cells or the potential alteration of cell characteristics by ex vivo expansion.

The identification of a marker combination that permits the isolation of primary MSCs enabled us to examine their physiological localization and role in the BM. We found that primary MSCs, with abundant Ang-1 expression, were predominantly in the arterial perivascular space near the inner surface of the bone, adjacent to vSMCs. Our data also demonstrated the in vivo fate of primary MSCs in a systemic transplantation assay. The transplanted primary MSCs (PαS cells) mainly differentiated into osteoblasts and Ang-1– and/or CXCL12-expressing perivascular cells, consistent with a recent study (Sacchetti et al., 2007). Collectively, our data conclusively demonstrate that primary MSCs and their descendants mainly function in the adult BM as a hematopoietic niche in the arterial perivascular area in BM (Doherty et al., 1998; Shi and Gronthos, 2003).

One of the most important observations of this study is that intravenously transplanted PαS cells were integrated not only into the BM but also into adipose tissue. Previous studies have largely indicated that MSCs are not transplantable. The systemic delivery of in vitro–isolated MSCs to recipient animals, although feasible, has been limited by the entrapment of donor cells in tissues, primarily the lungs, and the few successful transplantations were mostly performed by direct local or intralesional implantation (Miyahara et al., 2006; Muguruma et al., 2006).

As has been reported (Rombouts and Ploemacher, 2003), we found that cultured MSCs lost their homing ability. In addition, after ex vivo expansion, even the PαS cells were largely trapped in the lung (Fig. S4) and did not contribute to any BM compartment. Cell migration and tissue integration involve a cascade of events initiated by shear-resistant adhesive interactions between flowing cells and the vascular endothelium at the target tissue. This process is mediated by "homing receptors" expressed on circulating cells that engage relevant endothelial coreceptors, resulting in cell-tethering and rolling contacts on the endothelial surface; this is typically followed by chemokine-triggered activation of integrin adhesiveness, firm adhesion, and extravasation (Sackstein, 2005). The key molecule that mediates the homing capacity of primary MSCs is unknown, and its identification should be addressed in a future study. In addition, it is also possible that BM engrafted cells and CFU-Fs were derived from a distinct cell population because PαS cells still contain a heterogeneous population of cells. Thus, further purification and clonal transplantation studies would be necessary to prove our hypothesis.

Although cultured MSCs are multipotent in vitro, the cells often commit to the osteocyte lineage after local implantation (Sacchetti et al., 2007). We found that transplanted PαS cells that migrated to the BM mainly produced niche cells, as described above, but the cells that localized to adipose tissue differentiated into mature adipocytes. These results strongly suggested that primary MSCs can home to their appropriate niche and differentiate in response to cues from the local microenvironment. However, the discrepancy in differentiation potential between the in vitro and in vivo data remains to be addressed. In the in vitro differentiation assay,

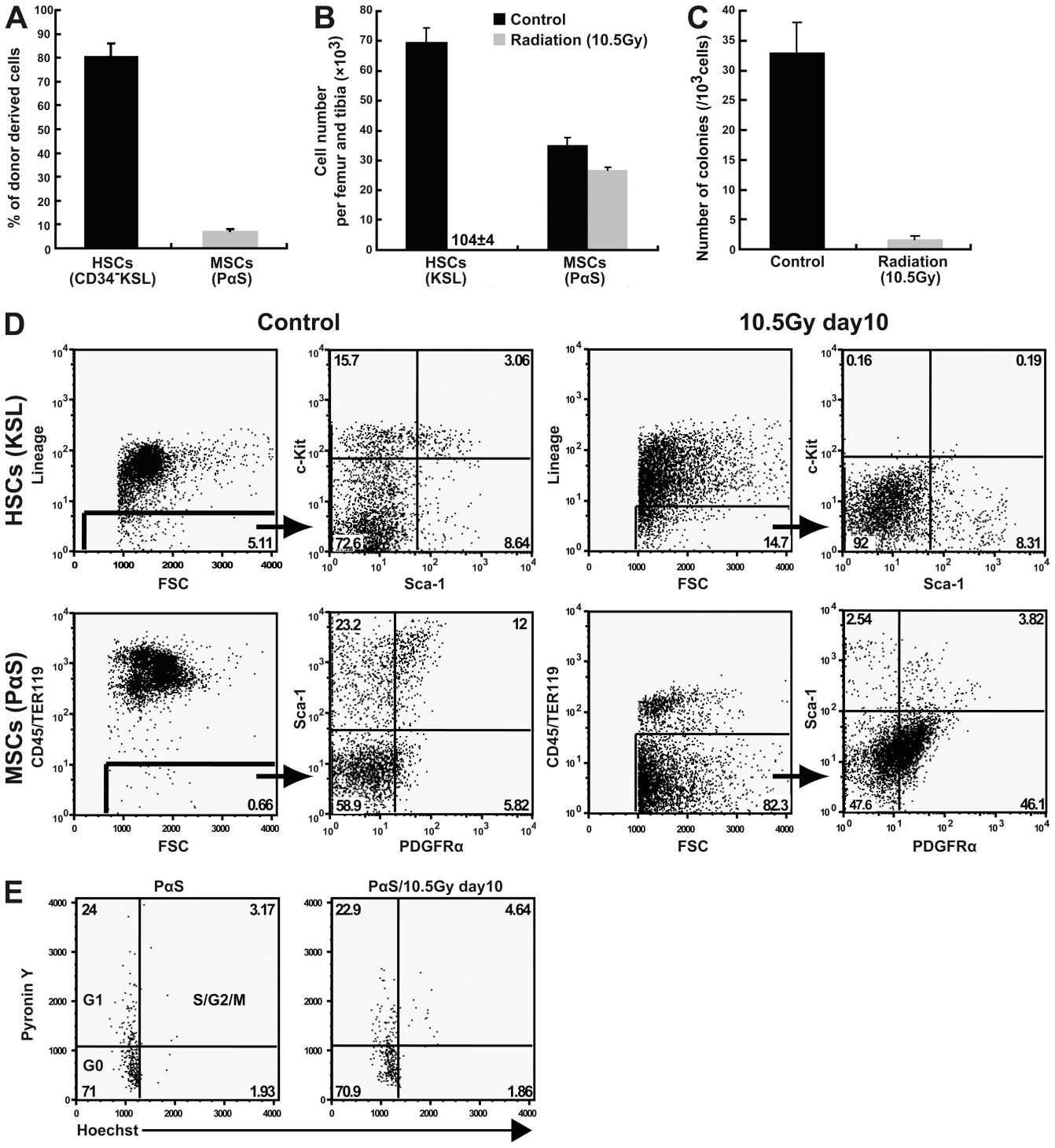

Figure 6. In vivo effects of lethal irradiation on the quiescence of PαS cells. HSCs ($CD34^{-}KSL$) from B6-Ly5.1 (CD45.1) mice and PαS cells (MSCs) from CAG-EGFP transgenic mice were transplanted together into lethally irradiated B6-Ly5.2 mice to examine the competitive repopulation of the appropriate niches. The graph shows the percentage of CD45.1 and GFP donor-derived cells detected in the BM of recipient mice 16 wk after transplantation (CD45.1, 81.1 ± 4.95%; GFP^{+}, 7.4 ± 0.40%.; $n = 3$ per group in three independent experiments). (B) The numbers of HSCs (KSL, $c\text{-}Kit^{+}Sca\text{-}1^{+}Lin^{-}$) and MSCs (PαS, $PDGFR\alpha^{+}Sca\text{-}1^{+}$) in the BM were calculated by ([Total number of BMMNCs] × [% of the cells] /100). Black bar, untreated control mice; gray bar, irradiated mice, 10 d after lethal irradiation. Results are means ± SEM ($n = 3$ per group). (C) The number of CFU-Fs formed from PαS cells isolated from either of unirradiated control (black) or lethally irradiated (Gray) wild-type C57BL/6. Means ± SEM ($n = 3$ per group). (D) Representative flow cytometric analysis of HSCs (KSL, top) or MSCs (PαS, bottom) in BMMNCs of lethally irradiated or unirradiated control mice. (E) Flow cytometry analysis of PY/Hoechst-stained PαS cells of unirradiated (left) and lethally irradiated (right) mice. Data are representative of three independent experiments.

single PαS-derived MSCs differentiated not only into chondrocytes and osteocytes, but also into endothelial cells and adipocytes. However, the primary PαS cells did not integrate into vSMCs in vivo. In addition, at least within 3 mo after transplantation, there were no detectable PαS-derived adipocytes in the BM. One explanation may be that naive MSCs are extremely sensitive to tissue level elasticity in the microenvironment and commit to specific lineages accordingly (Engler et al., 2006).

These findings have important clinical implications. Primary MSCs transplanted by systemic infusion may be useful for cell therapy of various systemic skeletal diseases, such as dyschondroplasia, osteochondrodysplasia, osteoporosis, and osteogenesis imperfecta. In contrast, local implantation is invasive and can result in significant morbidity, potentially disrupt the highly complex and delicate structure of the local regulatory microenvironment, and cause additional injury. Thus, stem cell–based therapy for systemic disorders mandates vascular delivery. However, this approach is limited by the difficulty of ensuring that sufficient numbers of reconstituting cells reach the damaged areas in cases of ineffective stem cell engraftment (Laver et al., 1987; Simmons et al., 1987; Agematsu and Nakahori, 1991; Awaya et al., 2002; Stute et al., 2002; Barbash et al., 2003; Meyerrose et al., 2007). Here, we demonstrated the detection of significant number of primary PαS-derived cells in the BM of transplant-recipient animals; however, the low engraftment activity of MSCs remains an unsolved problem. A key feature of stem cells is that they are in a quiescent state in vivo. Our results clearly revealed that >70% of PαS were in the G_0 phase, and the frequency of quiescent PαS in the BM did not change after lethal irradiation. These data demonstrate that although the radiation reduced the host CFU-F colony-forming ability in vitro, it did not physically kill the cells; instead, they remained alive, but mostly nonfunctional, in their niche. Finding nondeleterious ways to remove host MSCs, assuming that the cell cycle progression of transplanted MSCs can be induced, to expand the progenitor population and compensate for cell loss, will be our next challenge. If we succeed, freshly isolated MSCs could have great potential for correcting bone and BM-related systemic disorders.

Overall, the approach detailed here provides a means for researchers to study the therapeutic potential of cells from BM as a cell source for bone components and to elucidate how individual factors function in the control and maintenance of bone and BM formation in vivo and in a variety of health and disease states. Advances in this field hold promise for the development of rationale-based stem cell therapies for tissue regeneration and of gene therapy for inherited disorders.

MATERIALS AND METHODS

Mice

Adult wild-type C57BL/6 mice and B6.SJL-Ptprca Pep3b/BoyJ (C57BL/6-Ly5.1;Ly5.1) mice 8–12 wk of age were purchased from CLEA Japan, Inc. (Tokyo, Japan). Transgenic mice that ubiquitously express EGFP under the control of the CAG promoter (Kawamoto et al., 2000) were bred in our animal facility. The mice were kept under specific pathogen–free conditions in our animal facility at Keio University School of Medicine. All experimental procedures and protocols were approved by the ethics committee of Keio University and were in accordance with the Guide for the Care and Use of Laboratory Animals.

Preparation of BM cell suspension

Femurs and tibias were dissected and crushed with a pestle. The crushed bones were gently washed once in HBSS+ (Hanks-balanced salt solution supplemented with 2% FBS, 10 mM Hepes, and 1% penicillin/streptomycin), and the cell suspension filtered through a cell strainer (Falcon 2350) was discarded. The bone fragments were collected and incubated for 1 h at 37°C in 20 ml of DMEM (Invitrogen) containing 0.2% collagenase (Wako Chemicals USA, Inc.), 10 mM Hepes and 1% P/S. The suspension was filtered with a cell strainer (Falcon 2350) to remove debris and bone fragments, and collected by centrifugation at 280 *g* for 7 min at 4°C. The pellet was immersed in 1 ml water (Sigma-Aldrich) for 5–10 s to burst the red blood cells, after which 1 ml of 2× PBS (dilution from Sigma-Aldrich) containing 4% FBS was added, and the suspension was filtered through a cell strainer.

Antibody staining

The cells were suspended in ice-cold HBSS+ at 1–5 × 10^7 cells/ml, and then stained for 30 min on ice with the following mAbs: biotinylated or APC-conjugated PDGFRα (APA5), FITC-conjugated Sca-1 (Ly6A/E), PE-conjugated CD45 (30-F11), and TER119 (TER-119). Biotinylated antibodies were visualized with APC-conjugated streptavidin (Invitrogen). All mAbs were purchased from eBioscience. Flow cytometry analysis and sorting were performed on a triple-laser MoFlo (Dako) or FACSCalibur (BD) flow cytometer. PI fluorescence was measured, and a live cell gate was defined that excluded the cells positive for PI. Additional gates were defined as positive for PDGFRα and Sca-1 and negative for CD45 and TER119, according to the isotype control fluorescence intensity.

Cell culture

A variety of culture methods were required for this study, including adherent culture, CFU-F assay, cultures for MSC differentiation into mature cells, and CFU-C assay.

Adherent culture. Traditional MSC adherent culture was performed as described previously (Pittenger et al., 1999). Sorted cells were cultured in maintenance medium (i.e., MEMα + GlutaMAX-I [Invitrogen] supplemented with 10% FBS and antibiotics), incubated at 37°C with 5% CO_2, and maintained with exchanges into fresh medium every 3–4 d for 2–3 wk.

CFU-F assay. Approximately 1 × 10^3 or 2 × 10^3 sorted cells were seeded on a 100-mm dish in maintenance medium. Adherent cell clusters containing >50 cells were counted as a colony.

Differentiation cultures. To induce adipocyte differentiation, subconfluent cells were cultured with three cycles of Adipogenic Induction Medium/Adipogenic Maintenance Medium, with supplements from the Adipogenic Induction/Adipogenic Maintenance SingleQuot kit (Lonza). Each cycle consisted of feeding the subconfluent cells with the induction medium for 3 d, followed by 3 d of culture in the maintenance medium. After 14 d, the cells were fixed with 4% paraformaldehyde for 15 min, and stained with oil red O (MutoPure Chemicals).

For chondrogenic differentiation, cultured cells were harvested by trypsinization. The 2 × 10^4–2.5 × 10^5 cells were transferred into a 15-ml conical tube and washed with MEMα + GlutaMAX (Invitrogen). The tube was spun at 150 *g* for 5 min at room temperature, and the supernatant was aspirated. The cells were resuspended in 1 ml Differentiation Basal Medium Chondrogenic, with supplements from the Chondrogenic SingleQuot kit (Lonza), spun at 150×g for 5 min, and the medium was aspirated. The cells were resuspended in 1 ml of Differentiation Basal Medium Chondrogenic, supplemented with Chondrogenic SingleQuots kit, TGF-b3 (10 ng/ml; Lonza) and BMP-6 (500 ng/ml; R&D Systems), and spun at 150 *g* for 5 min at room temperature. The pellet was maintained with Differentiation Basal

Medium changes every 3–4 d for 3 wk. After 3 wk, cell clumps were harvested, washed in 4% paraformaldehyde, and stained with toluidine blue.

To induce osteocyte differentiation, subconfluent cells were cultured with Differentiation Basal Medium Osteogenic, supplemented with Osteogenic SingleQuots (Lonza) for 14 d. The cells were then fixed with 4% paraformaldehyde for 15 min and stained with alkaline phosphatase (Histofine; Nichirei).

For vasculogenesis, sorted cells were seeded on poly-L-ornithine/fibronectin (Sigma-Aldrich)-coated 8-well chamber slides (Iwaki) with Endothelial Cell Basal Medium-2 (EBM-2), supplemented with EGM-2 MV SingleQuots (Lonza), and incubated at 37°C with 5% CO^2. The cultures were maintained with medium changes every 4–7 d for 3 wk.

CFU-C assay. Cell suspensions were mixed with MethoCult (StemCell Technologies). Cells were plated in 35-mm dishes and cultured at 37°C with 5% CO_2. Colonies were scored on day 14.

Negative linear relationship assays

In this assay, the systematic dilution of cells reduces the plating cell density and increases the incidence of wells with no colonies. The sorted cells were seeded into 96- or 24-well plates or 100-mm dishes containing 14 cell-dose groups: 25; 50; 100; 200; 400; 500; 800; 5,000; 10,000; 50,000; 80,000; 1,000,000; 2,500,000; or 5,000,000 sorted cells per well. After 14 d, each well was fixed in methanol, stained with Giemsa, and the wells with no colonies were included in the count for each population. The concentration of cells plated in which 37% of the wells are negative for colony growth is the cell concentration that contains one CFU-F (Bacon and Sytkowski, 1987).

RT-PCR and quantitative RT-PCR (QRT-PCR) assay

RT-PCR was performed as described previously (Koide et al., 2007). The QRT-PCR assay was performed on an ABI 7500 Fast Real-Time PCR System using TaqMan Fast Universal PCR master mixture (Applied Biosystems) and TaqMan Gene Expression Assay Mix for Ang-1 (Mm00456503_m1) or CXCL-12 (Mm004455552_m1). The β-actin (actb) assay mix (Mm00607939_s1) served as an endogenous control. Data were analyzed by 7500 Fast System SDS Software 1.3.1. All experiments were done in quadruplicate.

In vivo transplantation

$CD34^-KSL$ cells (HSCs) from Ly5.1 congenic mice and PαS cells from CAG-EGFP transgenic mice were isolated as described above. Then, a mixture of 100 HSCs and 10^4 PαS cells were transplanted intravenously into the retro-orbital plexus of anesthetized recipient mice that had been lethally irradiated (10.5 Gy) along with 2×10^5 whole BM cells from recipient strain mice, as radioprotective cells.

Immunostaining of BM and adipose tissue

For BM and adipose tissue sections, whole-mount staining was performed as previously described (Kubota et al., 2008). The following antibodies were used as a primary antibodies; anti-GFP (rabbit IgG; 1:500; MBL; and goat IgG; 1:200; Santa Cruz Biotechnology, Inc.), α-SMA (1A4; FITC or Cy3-conjugated; Sigma-Aldrich), Sca-1 (D7; BD), PDGFRα (Santa Cruz Biotechnology, Inc.), Ang-1 (Santa Cruz Biotechnology, Inc.), CXCL12 (Abcam), osteocalcin (Santa Cruz Biotechnology, Inc.), and perilipin (Research Diagnostics). The secondary antibodies used were Alexa Fluor 488 fluorescence-conjugated IgGs (Invitrogen) or Cy3/Cy5-conjugated IgGs (Jackson ImmunoResearch Laboratories). For nuclear staining, specimens were treated with DAPI (Invitrogen).

Infection of lentivirus expressing firefly luciferase fused to Venus and preparation of transduced PαS cells

By using the fluorescent and luminescent fusion protein, the success of lentivirus infection was confirmed with fluorescent signal from Venus. After the transplantation, the spot(s) of transplanted PαS cells were followed by bioluminescent signal from Luciferin in mice body. Because we used the modified bioluminescent protein which emitted bigger bioluminescent signals than general one, only 10^5 cells could be detected easily. Sorted single PαS cell was cultured and proliferated, infected with lentivirus, continuously propagated, harvested, and then dissociated into single cells. The PI-negative/Venus-positive PαS cells were sorted by a flow cytometry and transplanted with HSCs (34-KSL).

BLI

We used a Xenogen-IVIS 100–cooled CCD optical macroscopic imaging system (SC BioScience Corporation) for BLI. For in vivo imaging, recipient mice transplanted with lentivirally engineered PαS cells were anesthetized and given D-luciferin (150 mg/kg body weight) i.p. We found this time window to be optimal because the signal intensity peaked at 15 min after administration followed by a plateau of 20 min (unpublished data). All images were analyzed as described in Materials and methods. To quantify the measured light, regions of interest (ROI) were defined as lungs and all values were examined from an equal ROI.

Statistical analysis.

The Tukey-Kramer test was used to compare the frequencies of CFU-Fs among different groups. All reported p-values were obtained using the SPSS software package (SPSS 15.0J for Windows).

Online supplemental material

Fig. S1 shows the quantification and differentiation of PαS cells isolated from different inbred mouse strains. Fig. S2 shows cell surface marker antigens of clonally cultured PαS cells. Fig. S3 is a schematic model of the physiological localization and behavior of MSCs in BM. Fig. S4 shows imaging of transplanted cultured MSCs in vivo. Table S1 lists primers used in this study. Table S2 lists monoclonal antibodies used in this study.Online supplemental material is available at http://www.jem.org/content/full/jem.20091046/DC1.

We thank Miyuki Ogawara and Takayuki Ohkawa for technical assistance and Lawrence Lein for proofreading this manuscript.

This work was supported by a grant from the Solution-Oriented Research for Science and Technology (SORST) program of the Japan Science and Technology Agency (JST) and from the Ministry of Education, Culture, Sports, Science and Technology (to H.O. and Y.M.), and also supported in part by a grant-in-aid from the Global Century COE program of the Ministry of Education, Science, and Culture of Japan to Keio University.

The authors have no conflicting financial interests.

Submitted: 12 May 2009
Accepted: 8 September 2009

REFERENCES

Agematsu, K., and Y. Nakahori. 1991. Recipient origin of bone marrow-derived fibroblastic stromal cells during all periods following bone marrow transplantation in humans. *Br. J. Haematol.* 79:359–365. doi:10.1111/j.1365-2141.1991.tb08041.x

Arai, F., A. Hirao, M. Ohmura, H. Sato, S. Matsuoka, K. Takubo, K. Ito, G.Y. Koh, and T. Suda. 2004. Tie2/angiopoietin-1 signaling regulates hematopoietic stem cell quiescence in the bone marrow niche. *Cell.* 118:149–161. doi:10.1016/j.cell.2004.07.004

Awaya, N., K. Rupert, E. Bryant, and B. Torok-Storb. 2002. Failure of adult marrow-derived stem cells to generate marrow stroma after successful hematopoietic stem cell transplantation. *Exp. Hematol.* 30:937–942. doi:10.1016/S0301-472X(02)00821-4

Bacon, E.R., and A.J. Sytkowski. 1987. Identification and characterization of a differentiation-specific antigen on normal and malignant murine erythroid cells. *Blood.* 69:103–108.

Barbash, I.M., P. Chouraqui, J. Baron, M.S. Feinberg, S. Etzion, A. Tessone, L. Miller, E. Guetta, D. Zipori, L.H. Kedes, et al. 2003. Systemic delivery of bone marrow-derived mesenchymal stem cells to the infarcted myocardium: feasibility, cell migration, and body distribution. *Circulation.* 108:863–868. doi:10.1161/01.CIR.0000084828.50310.6A

Beltrami, A.P., D. Cesselli, N. Bergamin, P. Marcon, S. Rigo, E. Puppato, F. D'Aurizio, R. Verardo, S. Piazza, A. Pignatelli, et al. 2007. Multipotent cells can be generated in vitro from several adult human organs (heart, liver, and bone marrow). *Blood*. 110:3438–3446. doi:10.1182/blood-2006-11-055566

Cho, C.H., Y.J. Koh, J. Han, H.K. Sung, H. Jong Lee, T. Morisada, R.A. Schwendener, R.A. Brekken, G. Kang, Y. Oike, et al. 2007. Angiogenic role of LYVE-1-positive macrophages in adipose tissue. *Circ. Res.* 100:e47–e57. doi:10.1161/01.RES.0000259564.92792.93

Conget, P.A., and J.J. Minguell. 1999. Phenotypical and functional properties of human bone marrow mesenchymal progenitor cells. *J. Cell. Physiol.* 181:67–73. doi:10.1002/(SICI)1097-4652(199910)181:1<67::AID-JCP7>3.0.CO;2-C

da Silva Meirelles, L., P.C. Chagastelles, and N.B. Nardi. 2006. Mesenchymal stem cells reside in virtually all post-natal organs and tissues. *J. Cell Sci.* 119:2204–2213. doi:10.1242/jcs.02932

Dezawa, M., H. Ishikawa, Y. Itokazu, T. Yoshihara, M. Hoshino, S. Takeda, C. Ide, and Y. Nabeshima. 2005. Bone marrow stromal cells generate muscle cells and repair muscle degeneration. *Science*. 309:314–317. doi:10.1126/science.1110364

Doherty, M.J., B.A. Ashton, S. Walsh, J.N. Beresford, M.E. Grant, and A.E. Canfield. 1998. Vascular pericytes express osteogenic potential in vitro and in vivo. *J. Bone Miner. Res.* 13:828–838. doi:10.1359/jbmr.1998.13.5.828

Engler, A.J., S. Sen, H.L. Sweeney, and D.E. Discher. 2006. Matrix elasticity directs stem cell lineage specification. *Cell*. 126:677–689. doi:10.1016/j.cell.2006.06.044

Friedenstein, A.J., U.F. Deriglasova, N.N. Kulagina, A.F. Panasuk, S.F. Rudakowa, E.A. Luriá, and I.A. Ruadkow. 1974. Precursors for fibroblasts in different populations of hematopoietic cells as detected by the in vitro colony assay method. *Exp. Hematol.* 2:83–92.

Goodell, M.A., K. Brose, G. Paradis, A.S. Conner, and R.C. Mulligan. 1996. Isolation and functional properties of murine hematopoietic stem cells that are replicating in vivo. *J. Exp. Med.* 183:1797–1806. doi:10.1084/jem.183.4.1797

Hoffmann, A., G. Pelled, G. Turgeman, P. Eberle, Y. Zilberman, H. Shinar, K. Keinan-Adamsky, A. Winkel, S. Shahab, G. Navon, et al. 2006. Neotendon formation induced by manipulation of the Smad8 signalling pathway in mesenchymal stem cells. *J. Clin. Invest.* 116:940–952. doi:10.1172/JCI22689

Hou, Z., Q. Nguyen, B. Frenkel, S.K. Nilsson, M. Milne, A.J. van Wijnen, J.L. Stein, P. Quesenberry, J.B. Lian, and G.S. Stein. 1999. Osteoblast-specific gene expression after transplantation of marrow cells: implications for skeletal gene therapy. *Proc. Natl. Acad. Sci. USA*. 96:7294–7299. doi:10.1073/pnas.96.13.7294

Jiang, Y., B.N. Jahagirdar, R.L. Reinhardt, R.E. Schwartz, C.D. Keene, X.R. Ortiz-Gonzalez, M. Reyes, T. Lenvik, T. Lund, M. Blackstad, et al. 2002. Pluripotency of mesenchymal stem cells derived from adult marrow. *Nature*. 418:41–49. doi:10.1038/nature00870

Jin, H.K., J.E. Carter, G.W. Huntley, and E.H. Schuchman. 2002. Intracerebral transplantation of mesenchymal stem cells into acid sphingomyelinase-deficient mice delays the onset of neurological abnormalities and extends their life span. *J. Clin. Invest.* 109:1183–1191.

Kawamoto, S., H. Niwa, F. Tashiro, S. Sano, G. Kondoh, J. Takeda, K. Tabayashi, and J. Miyazaki. 2000. A novel reporter mouse strain that expresses enhanced green fluorescent protein upon Cre-mediated recombination. *FEBS Lett.* 470:263–268. doi:10.1016/S0014-5793(00)01338-7

Kohyama, J., H. Abe, T. Shimazaki, A. Koizumi, K. Nakashima, S. Gojo, T. Taga, H. Okano, J. Hata, and A. Umezawa. 2001. Brain from bone: efficient "meta-differentiation" of marrow stroma-derived mature osteoblasts to neurons with Noggin or a demethylating agent. *Differentiation*. 68:235–244. doi:10.1046/j.1432-0436.2001.680411.x

Koide, Y., S. Morikawa, Y. Mabuchi, Y. Muguruma, E. Hiratsu, K. Hasegawa, M. Kobayashi, K. Ando, K. Kinjo, H. Okano, and Y. Matsuzaki. 2007. Two distinct stem cell lineages in murine bone marrow. *Stem Cells*. 25:1213–1221. doi:10.1634/stemcells.2006-0325

Kondo, T., S.A. Johnson, M.C. Yoder, R. Romand, and E. Hashino. 2005. Sonic hedgehog and retinoic acid synergistically promote sensory fate specification from bone marrow-derived pluripotent stem cells. *Proc. Natl. Acad. Sci. USA*. 102:4789–4794. doi:10.1073/pnas.0408239102

Kubota, Y., K. Takubo, and T. Suda. 2008. Bone marrow long label-retaining cells reside in the sinusoidal hypoxic niche. *Biochem. Biophys. Res. Commun.* 366:335–339. doi:10.1016/j.bbrc.2007.11.086

Laver, J., S.C. Jhanwar, R.J. O'Reilly, and H. Castro-Malaspina. 1987. Host origin of the human hematopoietic microenvironment following allogeneic bone marrow transplantation. *Blood*. 70:1966–1968.

Makino, S., K. Fukuda, S. Miyoshi, F. Konishi, H. Kodama, J. Pan, M. Sano, T. Takahashi, S. Hori, H. Abe, et al. 1999. Cardiomyocytes can be generated from marrow stromal cells in vitro. *J. Clin. Invest.* 103:697–705. doi:10.1172/JCI5298

Matsuzaki, Y., K. Kinjo, R.C. Mulligan, and H. Okano. 2004. Unexpectedly efficient homing capacity of purified murine hematopoietic stem cells. *Immunity*. 20:87–93. doi:10.1016/S1074-7613(03)00354-6

Meyerrose, T.E., D.A. De Ugarte, A.A. Hofling, P.E. Herrbrich, T.D. Cordonnier, L.D. Shultz, J.C. Eagon, L. Wirthlin, M.S. Sands, M.A. Hedrick, and J.A. Nolta. 2007. In vivo distribution of human adipose-derived mesenchymal stem cells in novel xenotransplantation models. *Stem Cells*. 25:220–227. doi:10.1634/stemcells.2006-0243

Miyahara, Y., N. Nagaya, M. Kataoka, B. Yanagawa, K. Tanaka, H. Hao, K. Ishino, H. Ishida, T. Shimizu, K. Kangawa, et al. 2006. Monolayered mesenchymal stem cells repair scarred myocardium after myocardial infarction. *Nat. Med.* 12:459–465. doi:10.1038/nm1391

Moore, K.A., and I.R. Lemischka. 2006. Stem cells and their niches. *Science*. 311:1880–1885. doi:10.1126/science.1110542

Morikawa, S., Y. Mabuchi, K. Niibe, S. Suzuki, N. Nagoshi, T. Sunabori, S. Shimmura, Y. Nagai, T. Nakagawa, H. Okano, and Y. Matsuzaki. 2009. Development of mesenchymal stem cells partially originate from the neural crest. *Biochem. Biophys. Res. Commun.* 379:1114–1119. doi:10.1016/j.bbrc.2009.01.031

Muguruma, Y., T. Yahata, H. Miyatake, T. Sato, T. Uno, J. Itoh, S. Kato, M. Ito, T. Hotta, and K. Ando. 2006. Reconstitution of the functional human hematopoietic microenvironment derived from human mesenchymal stem cells in the murine bone marrow compartment. *Blood*. 107:1878–1887. doi:10.1182/blood-2005-06-2211

Okada, S., K. Ishii, J. Yamane, A. Iwanami, T. Ikegami, H. Katoh, Y. Iwamoto, M. Nakamura, H. Miyoshi, H.J. Okano, et al. 2005. In vivo imaging of engrafted neural stem cells: its application in evaluating the optimal timing of transplantation for spinal cord injury. *FASEB J.* 19:1839–1841.

Ono, M., T. Maruyama, H. Masuda, T. Kajitani, T. Nagashima, T. Arase, M. Ito, K. Ohta, H. Uchida, H. Asada, et al. 2007. Side population in human uterine myometrium displays phenotypic and functional characteristics of myometrial stem cells. *Proc. Natl. Acad. Sci. USA*. 104:18700–18705. doi:10.1073/pnas.0704472104

Ortega, G., P.E. Korty, E.M. Shevach, and T.R. Malek. 1986. Role of Ly-6 in lymphocyte activation. I. Characterization of a monoclonal antibody to a nonpolymorphic Ly-6 specificity. *J. Immunol.* 137:3240–3246.

Osawa, M., K. Hanada, H. Hamada, and H. Nakauchi. 1996. Long-term lymphohematopoietic reconstitution by a single CD34-low/negative hematopoietic stem cell. *Science*. 273:242–245. doi:10.1126/science.273.5272.242

Oyama, T., T. Nagai, H. Wada, A.T. Naito, K. Matsuura, K. Iwanaga, T. Takahashi, M. Goto, Y. Mikami, N. Yasuda, et al. 2007. Cardiac side population cells have a potential to migrate and differentiate into cardiomyocytes in vitro and in vivo. *J. Cell Biol.* 176:329–341. doi:10.1083/jcb.200603014

Peister, A., J.A. Mellad, B.L. Larson, B.M. Hall, L.F. Gibson, and D.J. Prockop. 2004. Adult stem cells from bone marrow (MSCs) isolated from different strains of inbred mice vary in surface epitopes, rates of proliferation, and differentiation potential. *Blood*. 103:1662–1668. doi:10.1182/blood-2003-09-3070

Pereira, R.F., M.D. O'Hara, A.V. Laptev, K.W. Halford, M.D. Pollard, R. Class, D. Simon, K. Livezey, and D.J. Prockop. 1998. Marrow stromal cells as a source of progenitor cells for nonhematopoietic tissues in transgenic mice with a phenotype of osteogenesis imperfecta. *Proc. Natl. Acad. Sci. USA*. 95:1142–1147. doi:10.1073/pnas.95.3.1142

Phinney, D.G., G. Kopen, R.L. Isaacson, and D.J. Prockop. 1999. Plastic adherent stromal cells from the bone marrow of commonly used strains of inbred mice: variations in yield, growth, and differentiation. *J. Cell. Biochem.* 72:570–585. doi:10.1002/(SICI)1097-4644(19990315)72:4<570::AID-JCB12>3.0.CO;2-W

Pittenger, M.F., A.M. Mackay, S.C. Beck, R.K. Jaiswal, R. Douglas, J.D. Mosca, M.A. Moorman, D.W. Simonetti, S. Craig, and D.R. Marshak. 1999. Multilineage potential of adult human mesenchymal stem cells. *Science.* 284:143–147. doi:10.1126/science.284.5411.143

Prockop, D.J. 1997. Marrow stromal cells as stem cells for nonhematopoietic tissues. *Science.* 276:71–74. doi:10.1126/science.276.5309.71

Rombouts, W.J., and R.E. Ploemacher. 2003. Primary murine MSC show highly efficient homing to the bone marrow but lose homing ability following culture. *Leukemia.* 17:160–170. doi:10.1038/sj.leu.2402763

Sacchetti, B., A. Funari, S. Michienzi, S. Di Cesare, S. Piersanti, I. Saggio, E. Tagliafico, S. Ferrari, P.G. Robey, M. Riminucci, and P. Bianco. 2007. Self-renewing osteoprogenitors in bone marrow sinusoids can organize a hematopoietic microenvironment. *Cell.* 131:324–336. doi:10.1016/j.cell.2007.08.025

Sackstein, R. 2005. The lymphocyte homing receptors: gatekeepers of the multistep paradigm. *Curr. Opin. Hematol.* 12:444–450. doi:10.1097/01.moh.0000177827.78280.79

Sackstein, R., J.S. Merzaban, D.W. Cain, N.M. Dagia, J.A. Spencer, C.P. Lin, and R. Wohlgemuth. 2008. Ex vivo glycan engineering of CD44 programs human multipotent mesenchymal stromal cell trafficking to bone. *Nat. Med.* 14:181–187.

Shi, S., and S. Gronthos. 2003. Perivascular niche of postnatal mesenchymal stem cells in human bone marrow and dental pulp. *J. Bone Miner. Res.* 18:696–704. doi:10.1359/jbmr.2003.18.4.696

Simmons, P.J., D. Przepiorka, E.D. Thomas, and B. Torok-Storb. 1987. Host origin of marrow stromal cells following allogeneic bone marrow transplantation. *Nature.* 328:429–432. doi:10.1038/328429a0

Smith, L.G., I.L. Weissman, and S. Heimfeld. 1991. Clonal analysis of hematopoietic stem-cell differentiation in vivo. *Proc. Natl. Acad. Sci. USA.* 88:2788–2792. doi:10.1073/pnas.88.7.2788

Spangrude, G.J., D.M. Brooks, and D.B. Tumas. 1995. Long-term repopulation of irradiated mice with limiting numbers of purified hematopoietic stem cells: in vivo expansion of stem cell phenotype but not function. *Blood.* 85:1006–1016.

Stingl, J., P. Eirew, I. Ricketson, M. Shackleton, F. Vaillant, D. Choi, H.I. Li, and C.J. Eaves. 2006. Purification and unique properties of mammary epithelial stem cells. *Nature.* 439:993–997.

Stute, N., B. Fehse, J. Schröder, S. Arps, P. Adamietz, K.R. Held, and A.R. Zander. 2002. Human mesenchymal stem cells are not of donor origin in patients with severe aplastic anemia who underwent sex-mismatched allogeneic bone marrow transplant. *J. Hematother. Stem Cell Res.* 11:977–984. doi:10.1089/152581602321080646

Sugiyama, T., H. Kohara, M. Noda, and T. Nagasawa. 2006. Maintenance of the hematopoietic stem cell pool by CXCL12-CXCR4 chemokine signaling in bone marrow stromal cell niches. *Immunity.* 25:977–988. doi:10.1016/j.immuni.2006.10.016

Sun, S., Z. Guo, X. Xiao, B. Liu, X. Liu, P.H. Tang, and N. Mao. 2003. Isolation of mouse marrow mesenchymal progenitors by a novel and reliable method. *Stem Cells.* 21:527–535. doi:10.1634/stemcells.21-5-527

Takakura, N., H. Yoshida, Y. Ogura, H. Kataoka, S. Nishikawa, and S. Nishikawa. 1997. PDGFR alpha expression during mouse embryogenesis: immunolocalization analyzed by whole-mount immunohistostaining using the monoclonal anti-mouse PDGFR alpha antibody APA5. *J. Histochem. Cytochem.* 45:883–893.

Till, J., and E. McCulloch. 1961. A direct measurement of the radiation sensitivity of normal mouse bone marow cells. *Radiat. Res.* 14:213–222.

Wang, L., Y. Liu, Z. Kalajzic, X. Jiang, and D.W. Rowe. 2005. Heterogeneity of engrafted bone-lining cells after systemic and local transplantation. *Blood.* 106:3650–3657. doi:10.1182/blood-2005-02-0582